

PACS numbers: 52.25.Os; 52.50.Jm
DOI: 10.1070/QE2005v035n05ABEH003444

Laser plume spectroscopy. 1. Graphite target

V.V. Osipov, V.I. Solomonov, V.V. Platonov,
O.A. Snigireva, M.G. Ivanov, V.V. Lisenkov

Abstract. **Spectral and kinetic characteristics of a plume formed in the vicinity of a graphite target exposed to radiation from a pulsed CO_2 laser at 10.6 μm with a peak power of 9 kW (pulse energy 1.69 J, pulse duration 330 μs at the 0.1 level) in air are studied at room temperature. It is shown that the plume propagating at a right angle to the target surface and at an angle of 45° to the laser radiation is a nonequilibrium gas plasma flow at a temperature of the order of 10 kK; its shape and size are determined by the shape and power of the laser pulse. Emission of C^+ ions and C_2 molecules is excited in the plume. The temperature and emission are sustained by the energy of the exothermic reaction of association of carbon atoms and the vibrationally excited molecules formed in it.**

Keywords: *interaction of radiation with matter, laser plume, graphite target*.

1. Introduction

Evaporation of graphite by pulsed lasers [1–8] is widely used at present for depositing diamond-like films and obtaining nanosize tubes and powders. Despite the numerous investigations of the plasma produced upon laser evaporation, a generally accepted model has not been developed for a laser plume and the processes of condensation of a plasma plume into nanoparticles. It was assumed in [1, 3] that the target material enters the plume in the form of atomic vapour. However, the spectral lines of carbon atoms were discovered only in a plume produced upon irradiation of NiO-containing graphite by a KrF laser in an oxygen atmosphere at a pressure below 0.15 Torr [8]. Spectral lines of carbon atom were not detected in [4, 5, 7], but luminescence of C^+ ions as well as diatomic (C_2) and triatomic (C_3) carbon molecules was observed in the plume.

An intense broadband emission of the plume was observed at 510 nm upon excitation of graphite by a pulsed CO_2 laser in vacuum and by the second harmonic of a Nd laser in the argon atmosphere [5]. It was shown [4] that this emission band was the first to be observed, while spectral lines of the C^+ ions appeared only after tens of nanoseconds, followed by the Swann bands of the C_2 molecule. The broad band was attributed in [4] to the emission of incandescent carbon microparticles, but doubts were cast on this assumption in Ref. [5]. The emission spectrum of a plume observed upon excitation of graphite heated in air to a temperature of 1200 °C by a pulsed CO_2 laser represented a continuum with a maximum above 700 nm, which had a clearly manifested thermal (Planck) origin and a temperature below 4600 °C [7]. Based on this result, it was assumed in [9] that nanoparticles were produced already at the stage of the plasma plume expansion to the buffer gas (air).

The apparent discrepancy between the results presented above is probably due to the fact that they were obtained under different conditions. Most likely, this means that any significant variation in the characteristics of laser radiation producing a plume requires an independent investigation of its parameters. Therefore, the aim of our research is to carry out complex investigations of spatial spectral and kinetic parameters of the plume emission excited at a graphite target in air by a repetitively pulsed LAERT CO_2 laser [3].

2. Experimental

Figure 1 shows the scheme of the experimental setup. We used the same repetitively pulsed LAERT CO_2 laser as in [3, 9]. The multimode beam from this laser with a cross section of 3×4 cm was focused on plane graphite target (*1*) with the help of KCl lens (*7*) of focal length 10 cm. The target was exposed to laser radiation in air at room temperature. To prevent the laser pulse from falling into the same crater, the target was displaced mechanically after each pulse (except in special experiments).

Scanning of the laser plume along its length was performed with the help of quartz fibre (*4*) of diameter 1 mm, which transferred the optical flux to the entrance slit of spectral instrument (*5*) used for spectral and kinetic radiation measurements. The fibre was installed in focal plane (*3*) of quartz lens (*8*) with an 8-fold magnification of the plume image. Such a system provided a spatial resolution of at least 0.25 mm in spectral and kinetic measurements.

The emission spectrum of the plume in the range 350–800 nm was recorded during a single pulse using a diffraction spectrograph and a CCD multichannel photodetector connected to a computer. We measured the time-integrated intensity $I(\lambda) = \int_{t_0}^{T_0} I(\lambda, t)\mathrm{d}t$, where $T_0 = 10$ ms is

V.V. Osipov, V.I. Solomonov, V.V. Platonov, O.A. Snigireva, M.G. Ivanov, V.V. Lisenkov Institute of Electrophysics, Ural Branch, Russian Academy of Sciences, ul. Amundsena 106, 620216 Ekaterinburg, Russia; e-mail: plasma@iep.uran.ru, max@iep.uran.ru

Received 9 December 2004; revision received 18 March 2005
Kvantovaya Elektronika **35** (5) 467–473 (2005)
Translated by Ram Wadhwa

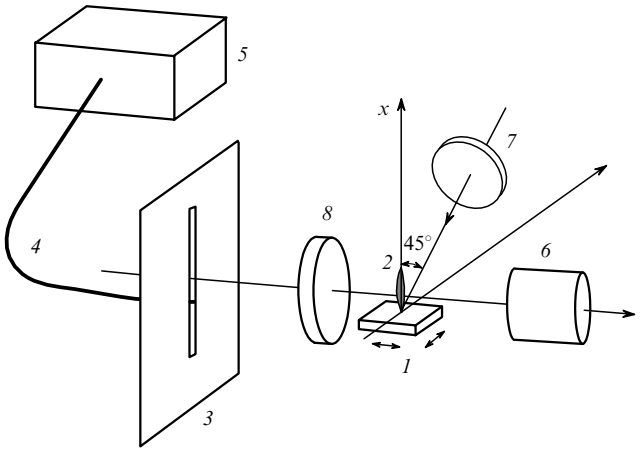

Figure 1. Scheme of the experimental setup: (*1*) graphite target; (*2*) laser plume; (*3*) focal plane of quartz lens (*8*); (*4*) optical fibre; (*5*) spectral instruments; (*6*) laser power meter; (*7*) KCl lens of focal length 10 cm.

the exposure time of the photodetector and t_0 is the time corresponding to the beginning of the integration, which coincides with the laser pulse onset to within 1 μs. The spectral data were averaged over 10 pulses. The wavelength measurement error did not exceed 0.75 nm, the instrumental function half-width was 2 nm, and the spectral resolution was about 2 nm. The wavelength calibration of the spectrum was performed using a mercury arc spectral lamp, while the intensity calibration was performed with the help of a standard incandescent lamp.

The emission kinetics $I(\lambda, t)$ was measured with the help of an MCD-1 monochromator equipped with a FEU-100 photomultiplier connected to a Tektronix-520A two-channel oscillograph with a pass band of 500 MHz. The wavelength was measured with an error of 2 nm by the monochromator with the same width of the instrumental function. To determine the time of appearance of the laser plume emission bands (with respect to the laser pulse onset), a signal from a pyroelectric detector of laser radiation and/or a pulse of the integrated plume radiation recorded with the help of FEK-22 was supplied to the second channel of the oscillograph. The synchronisation error was ±1 μs.

The spectral and kinetic characteristics of the plume were measured for a laser pulse incident on the target surface at an angle of 45°; the laser pulse energy being $W_{las} = 1.69$ J, power $P_{las} = 9$ kW, duration $t_{las} = 330$ μs at the 0.1 level and with a maximum at $t_m \approx 130$ μs. The finest nanopowders were obtained for these values of laser parameters [3]. The focal spot of laser radiation at the target was elliptical in shape with major and minor axes equal to 1.2 and 0.7 mm, respectively. In supplementary experiments, a VFU-1 high-speed movie camera was used to record the change in the geometry and brightness of the plume upon a variation of the energy, power and shape of the laser pulse, as well as the angle of its incidence.

3. Results of measurements

In all the measurements, the laser plume propagated at a right angle to the target surface. It was mushroom-shaped and consisted of a cylindrical column that was transformed into a cloud of irregular shape (typical time-resolved photographs of the plume are presented in [9]). While the shape of the laser pulse was preserved with increasing its power from 2.7 to 9 kW, a sharp increase was observed in the brightness of the plume, its total length (from 7 to 23 mm), the length of the column (from 5 to 14 mm), and the translational velocity of its propagation (from 40 to 110 m s^{-1}); the diameter of the column increased only slightly (in the range 1.5–1.8 mm). The time of achievement of the maximum length of the column remained virtually unchanged and coincided with the time $t_m \approx 130$ μs for which the laser pulse power achieved its maximum value The shape and the brightness of the plume varied insignificantly upon a change in the angle of incidence of the laser pulse from 90° to 45°. Spectral and kinetic studies revealed the formation of a crater of size 0.6×0.3 mm and a depth of about 5 μm on the target after its irradiation by a 9-kW laser pulse. This corresponds to the evaporation of 3.6–4.5 μg of carbon during one pulse.

Spectral measurements. Figure 2 shows the spectrograms of the plume emission, recorded at various distances from the target. The highest brightness was observed on the target surface (in the region $0 < l < 0.25$ mm). The spectrum exhibited two broad Gaussian bands with $\Delta\lambda = 102$ and 27 nm at 571 nm (17513 cm^{-1}) and 406 nm (24631 cm^{-1}), respectively (Fig. 2a), located on a wide pedestal. At a distance of $l = 0.25$ mm from the target, the integrated emission intensity decreased by a factor of 4.6 (Fig. 2b), and three Swann bands of the C_2 molecule ($d\,^3\Pi_g \rightarrow a\,^3\Pi_u$) were clearly observed, which were recorded earlier in [4, 5, 7]. The short-wavelength band corresponds to a transition involving a change $\Delta v = v_u - v_l = +1$ in the vibrational quantum number. This band consists of three bands corresponding to the 3–2 [469.6 nm (21295 cm^{-1})], 2–1 [470.9 nm (21236 cm^{-1}] and 1–0 [473.5 nm (21119 cm^{-1}] transitions. In the long-wavelength band ($\Delta v = v_u - v_l = -1$), the 2–3 [554.2 nm (18044 cm^{-1})] and 1–2 [558.5 nm (17905 cm^{-1})] transitions are most intense. The $\Delta v = v_u - v_l = 0$ band contains the intense 0–0 transition line at 516.3 nm (19369 cm^{-1}). The lines of the C^+ ion at 513.0, 511.9 and 514.3 nm (19493, 19535 and 19444 cm^{-1}, respectively), observed earlier in [4], are superimposed on this band. Also, a new strong narrow line was observed at 589.1 nm (16975 cm^{-1}). In addition, a broad short-wavelength band was observed at 406 nm (24631 cm^{-1}), which was observed separately and attributed to the emission of the C_3 molecule ($X\,^1\Sigma_g^+ \rightarrow A\,^1\Pi_u$) [10]. All these bands, lines and the broad pedestal were also preserved in the spectrum for the remaining plume regions. Upon moving away from the target, the following changes are observed in spectrum of the laser plume (Figs 2 and 3):

1. The spatial dependences of the intensities of all the bands and the pedestal (Fig. 3) are oscillatory in nature. The plume column is confined by two deep intensity minima for $l_1 \approx 0.6$ mm and $l_2 \approx 14$ mm, but a sharp local maximum is observed for $l = 6$ mm in the column for all the emission bands. Here the intensity $I(\lambda)$ of the Swann band at 516.0 nm becomes equal to the intensity at the target. However, the emission intensity $I = \int_{\lambda'}^{\lambda''} I(\lambda)\mathrm{d}\lambda$ integrated over the entire wavelength range from $\lambda' = 350$ nm to $\lambda'' = 800$ nm at this place in the plume is 2.2 times lower than at the target.

2. The intensity of the Swann bands of C_2 molecules, carbon ions C^+, and the pedestal vary according to the same law (Fig. 3).

3. Starting from $l = 5$ mm, two bands at 382.8 and 385.1 nm appear in the spectrum, which we interpreted as the

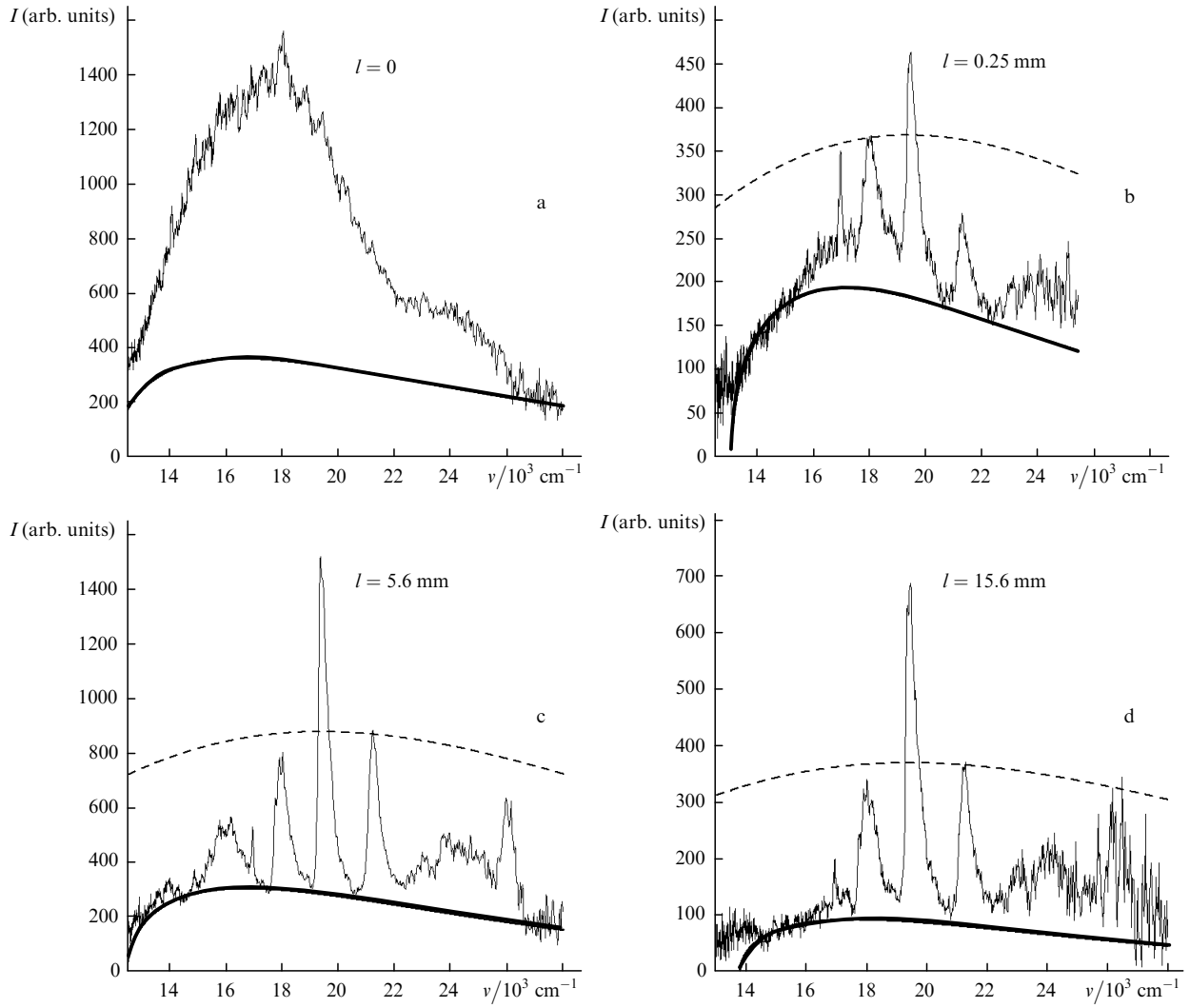

Figure 2. Emission spectra of the plume (thin solid curves) at various distances l from the target. Thick solid curves show the approximation of the recombination radiation while the dashed curves are the Planck curves.

Delander–D′Azambouk bands of the C_2 molecule ($C\,^1\Pi_g \rightarrow A\,^1\Pi_u$) corresponding to the 0–0 and 0–1 vibrational transitions, respectively. These bands appear within the plume column and their intensity achieves a maximum near $l = 6$ mm.

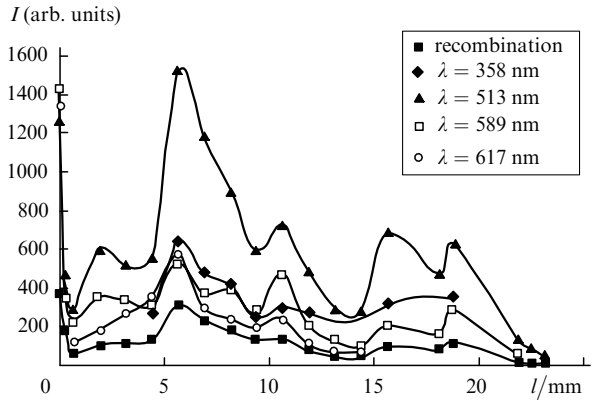

Figure 3. Dependence of the intensity $I(\lambda, l)$ on the distance l from the target for various spectral bands of the plume.

4. For $l > 3$ mm and right up to the end of the plume region, a structure with peaks at 416.5, 417.9 and 419.7 nm, which we assign to emission lines of the molecular nitrogen ion N_2^+ (the $B\,^2\Sigma_u^+ \rightarrow X\,^2\Sigma_g^+$ transition), is regularly observed in the region of the C_3 molecular band [11].

5. Beginning from $l > 3$ mm a highly structured band appears stochastically (not in each pulse) in the plume, in the interval 600–670 nm with peaks at 617.3, 632.2, 634.6 and 670.7 nm, which can be attributed to emission from highly excited levels of the first positive system of N_2 molecular bands. The stochastic nature of this band is also manifested during laser scanning of the graphite surface and in the case of irradiation of the same crater.

Kinetic measurements. The target surface begins to emit radiation simultaneously with the laser pulse onset (with an accuracy of 1 μs). Away from the target, the plume emission is delayed with respect to the laser pulse by a time t_d, which increases with l (Fig. 4). At the points in the plume at a distance $l < 9$ mm from the target (for $t < 80$ μs after the laser pulse onset), a local peak or intensity plateau is observed for all the bands. The main maximum is achieved at large times. Only one maximum is observed for $l > 9$ mm, the time of its appearance increasing with the distance of the point in the plume from the target. The subsequent decrease

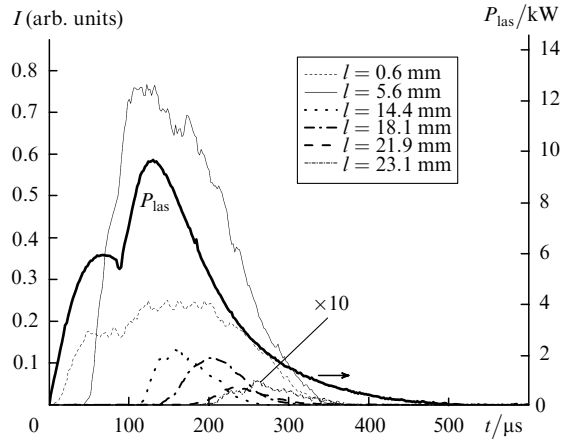

Figure 4. Kinetics of the intensities $I(t)$ of spectral bands and the laser pulse profile $P_{las}(t)$

in the intensities of all the bands occurs almost identically with a characteristic time considerably longer than the lifetime of the upper levels of optical transitions, as in Ref. [5]. Emission in all spectral bands and the pedestal at various points of the plume (in the column and the cloud) terminates almost simultaneously with the laser radiation pulse.

The delay times t_d are different for different spectral bands (Fig. 5). In particular, a regular tendency towards an earlier appearance of the pedestal and the 516-nm Swann band ($\Delta v = 0$) is observed, with the C^+ ion spectral lines at 513.0, 511.9 and 514.3 nm superimposed on it. Spectral bands of air molecules and triatomic carbon molecule are the last to appear.

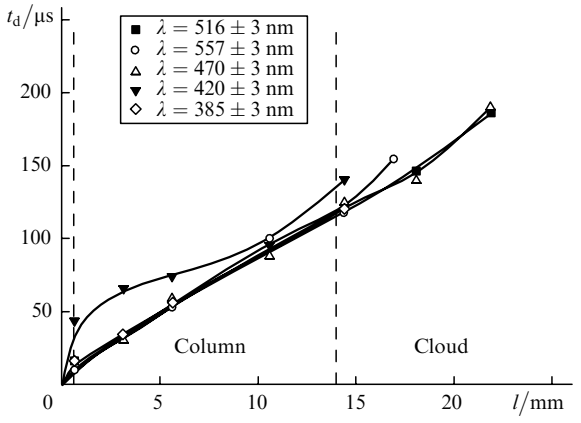

Figure 5. Dependence of the delay time t_d (at the 0.1 level) of emission from the laser plume at a distance l from the target.

An almost linear dependence of the delay time averaged over all the bands on the distance from the target l is observed in the laser plume column. A significant deviation from this dependence is observed in the plume cloud and in the vicinity of the target for $l < 0.6$ mm. Such a behaviour is a consequence of the translational propagation of the plume along the x axis (see Fig. 1). The velocity $V_f = l/t_d$ of the plume propagation increases near the target, becomes nearly constant (~ 110 m s^{-1}) in the plume column, and decreases monotonically in the cloud.

4. Discussion

Approximation of results. The continuous spectral band forming the pedestal is present at all points of the plume. The band shape (thin solid curve in Fig. 2) is well approximated by the curve describing the radiative recombination of ionised particles for the Maxwell energy distribution of free electrons:

$$I(h\nu) = \frac{a(h\nu - \Delta E)^{1/2}}{(kT_e)^{3/2}} \exp\left(-\frac{h\nu - \Delta E}{kT_e}\right), \quad (1)$$

where a is the normalisation factor and T_e is the electron temperature. In this reaction, photons with energy $h\nu = E + \Delta E$ are emitted, where E is the energy of a free electron and ΔE is the difference between the ionisation potential and the effective energy level of the particle formed upon recombination. Over the entire length of the plume, the difference ΔE remains unchanged ($\Delta E \approx 12700 \pm 300$ cm^{-1}), while T_e decreases from 15 kK at the beginning of the plume column to 10 kK at the end of the column.

At all points of the plume except $l = 0$, the envelope of the intensity maxima of the spectral bands is well described by the Planck curve (dashed curve in Fig. 2) with the distribution temperature $T_p \approx 10$ kK. The intensity of the 516-nm Swann band exceeds that of the envelope due to a purely 'instrumental' effect caused by the superposition of the instrumental profiles of closely spaced narrow lines from independent emitters of nearly the same intensity: C^+ ions (at 513.0, 511.9 and 514.3 nm) and C_2 molecules (at 516.3 and 512.9 nm). Because the interval between these lines is comparable with the half-width of the instrumental function ($\Delta\lambda = 2$ nm), a superposition of their instrumental profiles leads to an increase in total band intensity (Fig. 6).

It follows from the above approximation that the matter in the plume is almost in a state of equilibrium gas plasma with the temperature ~ 10 kK. Therefore, carbon nanoparticles cannot be formed in it.

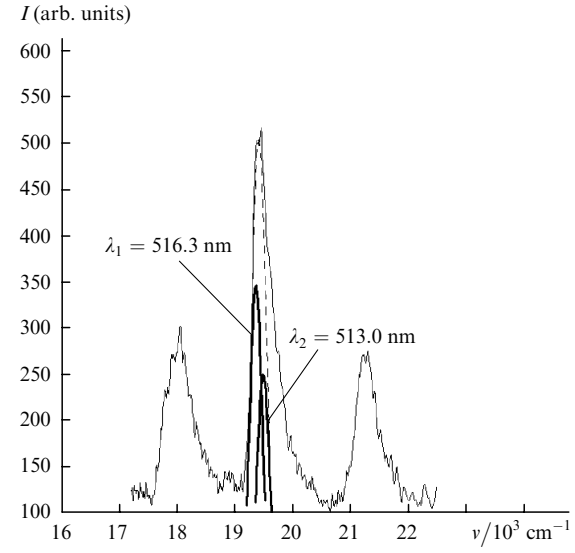

Figure 6. Influence of the instrumental function width on the measured spectral intensity (thin solid curve) in the Swann band region for $\lambda = 516$ nm. The solid curves show the instrumental profiles of the spectral lines of C^+ ion with $\lambda_1 = 513.0$ nm and C_2 molecule with $\lambda_2 = 516.3$ nm. The dashed curve shows their total profile.

Heating of the plasma plume. Plasma can be heated to a temperature of ~10 kK in the exothermic reaction of association of carbon atoms being evaporated from the target with the participation of a third particle M:

$$C + C + M \rightarrow C_2(v) + M. \quad (2)$$

Each event in this reaction is accompanied by the release of 6.2 eV. This energy is distributed among three internal (one vibrational and two rotational) and three translational degrees of freedom of the C_2 molecule being formed. As a result, the temperature of the molecules may rise by over 20 kK, i.e., more than what is observed in the experiments. First, this is explained by the energy exchange with colder particles not involved in reaction (2), second, by the fact that a part of the matter may escape from the target in the form of molecules and third, by the formation of molecules in highly excited vibrational states, which may lead to a vibrational temperature higher than the translational or rotational temperature. The degree of ionisation and dissociation of plasma can be estimated by using the relations following from the detailed balancing principle:

$$k_r n_e^2 = N^2 \sigma_m V_m \exp\left(-\frac{\varepsilon_i}{kT}\right), \quad (3)$$

$$N_C^2 k_a N = N^2 \sigma_m V_m \exp\left(-\frac{\varepsilon_d}{kT}\right). \quad (4)$$

The left-hand sides of these relations are the numbers of events of recombination (3) and association (4), while the right-hand sides are the numbers of events of ionisation (3) and dissociation (4) in a unit volume per unit time. Here N_C is the concentration of carbon atoms; k_r and k_a are the recombination and association constants; n_e is the electron concentration; N is the concentration of neutral molecules; σ_m is the gas-kinetic collision cross section; V_m is the mean velocity of random motion of molecules; $\varepsilon_i = 11.9$ eV and $\varepsilon_d = 6.2$ eV are the ionisation and dissociation energies. The association and dissociation reactions for carbon are identical from the energy point of view. Hence we can use for estimates the same values of rate constants for the reactions of recombination and association of carbon as for oxygen: $k_r \approx 10^{-7}$ cm^3 s^{-1} and $k_a \approx 10^{-31}$ cm^6 s^{-1} [12]. We assume that the plasma pressure in the plume is close to atmospheric. In this case, the concentration of heavy particles in the plasma is $N \approx 10^{18}$ cm^{-3} and will be $T_p/T_r \approx 33$ times lower than in air (T_r is the room temperature). It follows hence that $n_e \approx 10^{13} - 10^{14}$ cm^{-3} and $N_C \approx 10^{16} - 10^{17}$ cm^{-3} in the plume plasma.

The effect of laser radiation on the plume plasma parameters near the target was estimated by solving numerically the Boltzmann equation for electrons in a high-frequency electromagnetic field and calculating the kinetic constants of the processes involving electrons. It was found that the electron impact ionisation and dissociation rates are much lower than the corresponding rates of thermal processes.

Emission excitation mechanism. The emission bands of the plasma disappear over the entire length of the plume simultaneously with the end of the laser pulse (Fig. 4). This emission is sustained by the stored internal energy of C_2 molecules and partially by the external energy from the target resulted in reaction (2). The characteristic time of this reaction $\tau = (k_a N^2)^{-1} \approx 10^{-5}$ s (for $N = 10^{18}$ cm^{-3}) is long enough for reaction (2) to take place over the entire length of the plume. The electronically excited C_2^* molecules emitting Swann bands may be produced due to thermal excitation or inelastic energy exchange of vibrationally excited molecules formed directly in reaction (2).

C^+ emit at the $3p\,^4P \rightarrow 3s\,^4P^0$ (511.9 and 514.3 nm [4]), $3p\,^2P \rightarrow 4p\,^2P^0$ (513.0 nm), and $4p\,^2P^0 \rightarrow 3d\,^2D$ (589 nm) transitions. The upper levels of the first two transitions lie below the ground state of the C^{2+} ion by $\delta E = 10234$ and 14634 cm^{-1} respectively. The upper $4p\,^2P^0$ level of the third transition lies below the lower $3s\,^4P^0$ level of the first transition by $\delta E = 4440$ cm^{-1} (i.e., by a quantity of the order of kT). The upper levels of the first two transitions can be excited during recombination of the doubly charged C^{2+} ions. However, the formation of such ions in the plume is unlikely. The presence of highly excited C^+ ions in the plasma is due to the cascade transmission of energy from the electronically excited C_2^* molecule. Indeed, the plume plasma contains C^+ ions whose concentration is maintained at the level $(1-4)(N_{C_2^+} N_C/N) \approx 10^{13} - 10^{14}$ cm^{-3} due to a charge exchange between C^{2+} and C^+ ions.

In turn, the radiative recombination of C^{2+} and C^+ ions forms a pedestal in the emission spectrum of the plume. It can be assumed that the main contribution to the pedestal comes from the radiative recombination of ions. This assumption is based on the fact that only this reaction can produce carbon atoms that are predominantly in the $4s\,^3P^0$ state with an energy differing from the ionisation energy by $\delta E = 12773 - 12730$ cm^{-1}; this is in good agreement with the approximate value $\Delta E \approx 12700 \pm 300$ cm^{-1}. The absence of carbon emission lines in the spectrum is explained primarily by the fact that these lines are located in the UV spectral region and are not detected by our instruments, and also because of a strong competition with reaction (2).

Plume propagation. The size of the plume and its emission intensity are determined by the plasma flux from the target region and the rate of its recombination. In the one-dimensional approximation, the expression for the change in the concentration N_C of carbon atoms whose association eventually leads to plasma excitation can be written at each point ($x = l$) in the plume in the form

$$\frac{dN_C}{dt} = f(t) - \frac{N_C}{\tau}, \quad (5)$$

where $\tau = 10^{-5}$ s is the effective characteristic time of reaction (2); $f(t)$ is a function describing the supply of carbon atoms to the point ($x = l$) from the target. The function $f(t)$ is determined by the shape of the laser pulse $P_{las}(t)$ and can be represented in the form

$$f(t) = \begin{cases} P_{las}(t) w(x,t), & t_d < t < t_{las}, \\ 0, & t < t_d, t > t_{las}, \end{cases} \quad (6)$$

where t_d is the time of appearance of plasma at the point $x = l$; t_{las} is the duration of the laser pulse at the base; and $w(x,t)$ is the 'scattering' function taking into account the laser radiation power losses not connected with the formation and transportation of plasma. One can see that if the value of τ is much smaller than the characteristic time of variation of laser pulse power (10^{-4} s), the change in the concentration of particles [except for the factor

$w(x,t)$] coincides with the form of the laser pulse. This conclusion is confirmed by the fact that if the target is exposed to a laser pulse with a single peak, the kinetics of the intensities of all bands displays only one peak for all values of l.

Characteristic plume regions. Let us use the model described above to analyse the behaviour of the spectral kinetic parameters in the plume. Three regions with quite different emission parameters are distinguished in the plume: the region near the target surface ($l \leqslant 0.6$ mm), the plasma column (0.6 mm $< l \leqslant 14$ mm) with an extremal point at $l = 5.6$ mm, and the head (cloud) at 23 mm $> l > 14$ mm.

A bright emission whose spectrum exhibits (see Fig. 2) two Gaussian broad bands on a wide pedestal appears in the immediate vicinity of the target surface ($l = 0$). The pedestal corresponds to recombination radiation and is well described by expression (1). For $\Delta E \approx 12800$ cm^{-1} and $T_e \approx 15$ kK, the pedestal has the maximum height and the deviation of the emission spectrum from the Planck curve is the strongest (see Fig. 2). The brightest Gaussian band corresponds to the system of Swann bands and the 'high-pressure band system' (vibronic transitions with $|\Delta v| > 1$) in the C_2 molecule. The second band corresponds to the radiation emitted by the C_3 molecule. The formation of the Gaussian profile may be related only with the overlap of strongly broadened vibronic lines (up to $\Delta\lambda \approx 1$ nm) for a particle concentration $n_1 > 10^{20}$ cm^{-3}. Such a concentration may be achieved in a surface layer having a thickness of the order of half the laser radiation wavelength ($l \approx 5$ mm) during the action of the laser pulse. A high-pressure plasma ($p_1 = n_1 k T_1$) is formed in this layer and expands under the action of this pressure in the vicinity of the target of size not exceeding 0.6 mm. The internal pressure $p_2 = n_2 k T_2$ of the plasma is approximately balanced by the external air pressure $p_a = n_L k T_r$ (n_L is the Loschmidt number), the temperature and concentration n_2 decrease to 10 kK and $\sim 10^{18}$ cm^{-3} respectively. During adiabatic ($V T^{(\chi-1)^{-1}} =$ const) expansion of the plasma consisting predominantly of diatomic molecules ($\chi = 4/3$), its initial concentration n_1 must be close to 10^{20} cm^{-3} while its temperature must be ~ 25 kK.

In the column of the plume ($l > 0.6$ mm), the plasma propagates with a constant translational velocity $V_f = l/t_d \approx 110$ m s^{-1}, expelling the surrounding air. Therefore, the emission spectrum of the column does not contain the band corresponding to the atmospheric air for $l < 3$ mm, and only emission bands of the C^+ atomic ion and of C_2 and C_3 molecules are observed. These bands are well resolved and their intensity at the beginning of the column (for $l = 0.6$ mm) is about an order of magnitude lower than the intensity in the vicinity of the target, which points towards a sharp decrease in the plasma concentration. However, the electron and plasma ion temperatures estimated from formula (1) and the Planck formula do not change significantly. The temperature is sustained due to heating of particles in reaction (2) and dissipation of the vibrational energy of C_2 molecules. The maximum length ($l = 14.4$ mm) of the plume column is attained at the instant $t_d \approx 130$ μs corresponding to the peak laser pulse power (see Fig. 4). This means that the column is formed during building up of the laser pulse power. It is the power build-up that ensures a dynamic equilibrium between the plasma pressure and the air drag. As a result, the velocity of translational motion of the plasma remains constant and its specific value is determined by the laser power build-up rate. This conclusion is confirmed in experiments in which the laser pulse power decreases while its shape is preserved.

In our experiments, the laser pulse had two distinct local maxima (Fig. 4). By the time the first maximum was attained ($t_d \approx 55$ μs), the column length was 6 mm. The highest intensity for all spectral lines and the pedestal were attained at this stage. The emergence of the maximum is associated with the decrease in the ordered motion pulse of the plasma associated with a decrease in the laser pulse power. This leads to a local trapping of the molecules of the surrounding gas and an increase in the plasma density manifested in the form of random luminescence spikes for air molecules.

For $l > 14.4$ mm ($t_d \approx 130$ μs), the plasma movement slows down once again, diffusive blurring of the plume (cloud formation) takes place, and the emission intensity increases. As in the plasma column, emission with a band spectrum is observed in the cloud until the termination of the laser pulse. The temperature of the gas and the electrons remains quite high during emission. After termination of emission with a band spectrum, a weaker structureless thermal radiation persists in the cloud for a long time (up to 500 μs).

5. Conclusions

We have shown that a laser plume produced upon irradiation of a graphite target by a 9-kW pulsed CO_2 laser is a nearly equilibrium plasma flow with a temperature of heavy particles of the order of 10 kK. This temperature and emission with a band spectrum are sustained by the energy of the exothermic reaction of association of carbon atoms and of the vibrationally excited molecules formed in it.

As the laser pulse power increases, the plume propagates in the form of a narrow cylindrical column at a nearly constant velocity at a right angle to the target surface. Upon a decrease in the laser power, the velocity of the plume decreases, the nature of its propagation becomes unstable, and an irregularly shaped cloud is formed at the end of the column. The shape and size of the column and plume cloud are determined by the shape of the laser pulse. Emission with a band spectrum is observed in the plume only during the action of a laser pulse.

During the action of the laser radiation, a dense plasma with a temperature $\sim 10 - 25$ kK, which is much higher than the temperature of sublimation of graphite ($T = 4.5$ kK) is formed in the vicinity of the target. Obviously, the presence of this plasma must exert a considerable influence on the entire process of evaporation of graphite. The analysis of this phenomenon forms the subject matter of detailed investigations.

During the action of a laser pulse of power exceeding 2.7 kW, and in the presence of bands and lines of carbon atoms and molecules in the emission spectrum of the plume, the probability of their condensation into solid particles is low due to a high temperature of the plasma. Solid particles are formed after cooling of the plasma, mainly in the region of the plume cloud. On account of the large size of this region, the concentration of carbon atoms and molecules in it is low and hence the probability of formation of large solid particles is also low.

Acknowledgements. This work was partly supported by

INTAS (Project No. 03-51-3332) and the Presidium of the Ural Branch of the Russian Academy of Sciences ('Generation of High-Power Laser Radiation And Its Applications For Developing New Technologies' under the programme of integration of Ural and Siberian Branches of the Russian Academy of Sciences). One of the authors (M.G. Ivanov) acknowledges the support of the Russian Science Support Foundation and the Ural Branch of the Russian Academy of Sciences.

References

1. Muller E., Oestreih Ch., Popp U., et al. *J. KONA – Powder and Particle*, (13), 79 (1995).
2. Popp U., Herbig R., Michel G., et al. *J. European Ceramic Soc.*, **18**, 1153 (1998).
3. Kotov Yu.A., Osipov V.V., Ivanov M.G., et al. *Zh. Tekh. Fiz.*, **72** (11), 76 (2002).
4. Dem'yanenko A.V., Letokhov V.S., Puretskii A.A., Ryabov E.A. *Kvantovaya Elektron.*, **25**, 36 (1998) [*Quantum Electron.*, **28**, 33 (1998)].
5. Arepalli S., Scott C.D. *Chem. Phys. Lett.*, **302**, 139 (1999).
6. Kokai F., Takahashi K., Yudasaka M., et al. *J. Phys. D: Appl. Phys.*, **33**, 545 (2000).
7. Kokai F., Takahashi K., Kasuya D., et al. *Appl. Phys. A*, **73**, 401 (2001).
8. Nakajima K., Furusava M., Yamamoto T., et al. *Diamond and Related Materials*, **11**, 953 (2002).
9. Mesyats G.A., Osipov V.V., Volkov N.B., et al. *Pis'ma Zh. Tekh. Fiz.*, **29** (18), 54 (2003).
10. Monchicourt P. *Phys. Rev. Lett.*, **66**, 1430 (1991).
11. Lipchak A.I., Solomonov V.I., Tel'nov V.A., Osipov V.V. *Kvantovaya Elektron.*, **22**, 367 (1995) [*Quantum Electron.*, **25**, 347 (1995)].
12. Hokazono H., Fujimoto H. *J. Appl. Phys.*, **62**, 1585 (1987).